Structural, Thermal, and Electrical Behavior of Tin-aluminum Alloy Modified with Indium

Feryal DAWOOD [1], Abbas AL-BAWEE [2], Ahmed ALRUBAIY [2] *, Abeer SHEHAB [2]

[1] *University of Diyala, College of Basic Education, Old Baghdad Street, Al-Mouradia, Baquba, Diyala Governorate, 32001 Iraq*
[2] *University of Diyala, College of Engineering, Al Qudis Square, Baquba, Diyala Governorate, 32002, Iraq*

http://doi.org/10.5755/j02.ms.44672

Received 31 March 2026; accepted 2 June 2026

Lead-free solder alloys are crucial in the electronics production sector due to environmental and health concerns. While tin aluminum alloys are good alternatives, the addition of indium improves their properties. This study investigates the effect of indium addition on the structural, thermal, and electrical properties of tin aluminum alloys. $Sn_{95-x}Al_5In_x$ alloys (where x = 5, 10, and 15 wt.%) were made, and examined using X-ray diffraction, scanning electron microscopy and differential scanning calorimetry. The mechanical, electrical and thermal properties were measured. The addition of indium caused changes in the microstructure and the formation of intermetallic compounds. The Vickers hardness increased from 36.43 kg/mm² for $Sn_{95}Al_5$ alloys to 38.92 kg/mm² for $Sn_{80}Al_5In_{15}$ alloys, while the modulus of elasticity increased from 31.71 GPa to 37.92 GPa with increasing indium content. The melting temperature decreased by up to 130 °C, while mechanical strength and hardness varied with indium content. Electrical resistivity showed variations depending on indium concentration as well. This work is notable for investigating the change in electrical resistivity with varying indium content, highlighting the important role of indium in modifying these properties. The results demonstrate that tin-aluminum-indium alloys exhibit modified melting points and improved mechanical properties, suggesting their potential use in lead-free welding applications and improved welding efficiency.
Keywords: thermal properties, melting temperature, lead-free solder, electrical resistivity, indium addition.

1. INTRODUCTION

Due to increasing demand, driven by regulatory requirements and consumer preferences, for reliable, lead-free alternatives, lead-free solder alloys have become crucial in the digital hardware Industry for their environmental and health benefits. Given their potential high performance, eutectic tin-aluminum (Sn-Al) systems have garnered significant attention [1]. However, tin-aluminum alloys suffer from certain limitations, including their high melting point and coarse microstructure, which affect their mechanical strength and reliability. Research by Al Katawy et al. [2] explores one method for improving alloy properties through austenitic quenching using a molten bismuth-gallium alloy, while this study focuses on the use of indium as an additive to enhance tin-aluminum systems for electronics soldering operations.

Indium (In), a versatile element, improves the thermal and structural properties of tin-aluminum alloys [1, 3]. However, tin-aluminum binary systems with eutectic structures are characterized by high melting points and coarse microstructures, which limit their performance. Therefore, the addition of indium lowers the melting points of these alloys and improves their grain structure. Indium can form unique intermetallic phases that enhance electrical, mechanical, and thermal properties [4]. The benefits of indium in other welding systems (tin-bismuth and tin-silver-copper) are well-known and documented, but its role in tin-aluminum alloys has not been adequately studied. There is significant lack of knowledge regarding the effect of indium concentration on electrical resistance, thermal stability and microstructure in tin-aluminum-indium alloys. Increasing the indium content significantly improves mechanical strength, and toughness, but excessive use can reduce electrical conductivity due to the increased presence of intermediate metals. For example, tertiary alloys of tin, aluminum, and zinc, containing approximately 15 % indium are showing promise in lead-free welding, exhibiting excellent overall performance [5].

The microstructure and thermal properties of aluminum alloys are significantly influenced by the addition of indium. For example, it helps create different types of solid particles as the metal cools, resulting in smaller and more evenly sized grains instead of large column-like grains. By improving the precipitation behavior of phases, the addition of indium improves the alloy's ductility, hardness, and yield strength [3]. It also has an impact on the temperature at which substantial precipitation happens, which influences the distribution and solubility of other alloying elements. However, indium clustering may cause the alloy's microstructure to be non-uniform, which could have an effect on its long-term performance and stability [1].

Since indium addition plays a key role in improving the grain structures of tin-aluminum alloys it is crucial for the development of alloys. Instead of producing coarse columnar grains, it causes heterogeneous nucleation during solidification, resulting in the formation of fine uniformly sized grains. This is because indium can lower the melting

* Corresponding author: A. Alrubaiy
E-mail: *Ahmed_ail_eng@uodiyala.edu.iq*

point of the alloy and increase the rate of nucleation as shown in the study by Chen and Yan [6]. The formation of Al grains is aided by the nucleation sites created by indium atoms in the alloy melt, which encourage the development of fine grains. Smaller grains are produced as a result of easier nucleation. The addition of indium has been shown to reduce the average grain size by up to 83 % (Chen & Yan, 2020; Mostafa, 2019) [6]. Similarly, Dawood et al. [7] reported that incorporating 2 wt.% In into $Sn_{43}Bi$ solder alloys decreased the particle size from 465.58 Å to 217.09 Å, confirming indium's strong grain refinement effect through microstructural regulation. The addition of elements like boron and titanium to indium increases the effect of fine-grain refinement. By adding nucleation sites this produces particles like Al_3Ti and TiB_2 which leads to a finer grain structure [8]. In general, the incorporation of indium is essential for the development of alloys, and the composition of alloys.

The addition of indium, which results in the formation of various phases, has a significant impact on the mechanical properties of aluminum alloys. The formation of phase precipitates that are more densely and finely distributed results from the addition of indium to aluminum alloys which changes the precipitation process. Peak hardness rises significantly as a result [9]. Similar microstructural transformations have been observed in aluminum alloys, where grain refinement and hardness improvements occur through mechanical processing [10]. Indium atoms and vacancies have a high binding energy, which results in the suppression of unwanted phases like GP zones. The formation of more desirable phases is induced by indium which results in improved mechanical properties [11]. The composition of deposits in alloys is affected by the presence of indium, which leads to the formation of finer-phase deposits with higher number densities in aluminum and copper alloys, resulting in improved hardness and yield strength [12]. Thermomechanical treatments can significantly alter the microstructure and mechanical properties of aluminum alloys, highlighting the need for improvements in microstructural engineering [10]. Improving the grain structure and forming fine deposits as a result of adding indium creates a synergistic effect on the mechanical performance of aluminum alloys, which in turn leads to increased hardness, strength, and flexibility. According to Akopyan et al. [9], the addition of indium to Al-Si-Cu alloys results in a 22 % increase in peak hardness and a 15-fold increase in yield strength. Furthermore, the alloy's thermal stability is improved by the addition of indium as the more refined precipitates and finer grain structure resist coarsening during high temperature exposure thereby preserving the alloy's strength at elevated temperatures [12].

Essential trace element indium greatly affects the precipitation behavior of phases in tin-aluminum alloys. The change of the precipitation dynamics maximizes the mechanical characteristics of these alloys by improving some phases and restricting others. Indium changes the microstructure of tin-rich alloys, especially in grain boundary wetting transitions, which can raise the alloys' electrical conductivity [13]. The settling behavior of a particle in tin-aluminum alloys is much influenced by the way indium clusters in aluminum. The inclination of indium atoms to form clusters which act as nucleation sites for precipitates affects the alloy's general precipitation kinetics and microstructure. Indium clustering creates localized areas in aluminum alloys that help precipitates like Al3(Sc,Zr) to form.

In indium-containing alloys, microhardness gradually increases over time, and creep rates decrease, which in turn improves performance under stress [14]. Indium significantly affects the deposition temperature, leading to agglomeration at lower temperatures. Thus, indium agglomeration negatively affects the solubility and distribution of other alloying elements [11]. While indium accelerates the precipitation process, it can simultaneously lead to inconsistent microstructures, affecting the alloy's stability and effectiveness over time and under changing conditions.

Indium significantly increases the thermal conductivity of tin-aluminum alloys, with $SnBi_{43}In_2$ exhibiting the highest recorded thermal conductivity of 24 W/m·K [7]. Adding indium to tin alloys not only changes the chemical composition but also maps the microstructure, which is the underlying basis for thermal performance. This is also influenced by elements such as copper and silver, and the tin-to-aluminum ratio [15]. In small samples, the alloys can be homogenized and tempered to improve the structure and enhance thermal properties [16]. However, precise temperature control becomes challenging and understanding the interrelationships between elements is crucial for high-performance thermal systems [17]. Improved thermal conductivity in tin-indium alloys is critical for the efficient terminating of high-power electronic components without thermal breakdown [18]. However, in Sn-Al-In alloys, indium tends to agglomerate, disrupting the thermal distribution and destroying phase stability, which renders the alloy unreliable in advanced cooling systems [19]. Therefore, every change in the microstructure alters the thermal properties, and control requires fine-tuning and continuous improvement.

Temperature significantly affects the tin-indium alloys, and their thermal conductivity particularly related the concentration of indium present. When the indium concentration is below 3 % a linear correlation with temperature is observed spanning approximately 5 to 17 K, primarily attributed to phonon scattering. The addition of indium, particularly in its liquid state enhances thermal conductivity. This effect continues even at high temperatures reaching up to 1173 K as indicated by Stankus et al. [20]. Regardless of the alloys state, whether solid or liquid, thermal conductivity generally increases with temperature, exhibiting a linear correlation with high temperatures. Alloys with a higher concentration of indium exhibit superior thermal conductivity. Liquid indium-tin alloys are markedly more efficient than their solid equivalents [20, 21]. However, these properties can also be affected by the distinct microstructural characteristics of the alloy. This indicates that under varying conditions, thermal performance may differ.

The structural, thermal, and electrical properties of tin-aluminum alloys are significantly affected by the addition of indium, which leads to a change in their characteristics in multiple dimensions. It has a direct impact on the alloy's thermal stability, electrical resistivity and structural

integrity. The crystalline structure of tin-aluminum alloys is affected by the addition of indium, which results in modifications to grain boundaries and lattice parameters [22, 23]. Mechanical properties are improved by variations in crystal size and phase formation, resulting in a more refined microstructure [24]. Therefore, the addition is essential for a variety of applications because of its ability to modify electrical resistivity, enhance thermal stability, and alter the microstructure.

The thermal properties of tin-aluminum alloys are enhanced by the addition of indium, which results in a reduction in specific heat and melting temperature, suggesting improved thermal management [25]. Alhumairi et al [19] observed that thermal stability correlates with material composition, a finding that parallels the reduced melting temperatures, and altered thermal conductivity in Sn-Al-In alloys. The thermal conductivity of tin-aluminum alloys is contingent upon the quantity of indium present. The thermal conductivity of the alloy could range from 60.60 to 188.50 W/Km contingent upon its composition [26]. Kim et al. [24] have demonstrated that the alloy is well-suited for high-temperature applications because of its improved thermal stability.

The electrical resistivity of tin-aluminum alloys increases when they contain a greater amount of indium. This is because indium is dispersed throughout the matrix [22, 27]. The resistivity values can fluctuate significantly depending on the alloy composition and treatment [26]. Bakhtiyarov [27] have emphasized the importance of indium distribution through the alloy matrix as it directly influences conductivity and signals the onset of the sedimentation process. But the incorporation of indium may present obstacles, such as an increase in resistivity that could affect the conductivity in specific applications. So, it is imperative to achieve the balance between these effects to optimize the performance of the alloys, which contain indium.

Tin-aluminum alloys exhibit improved thermal conductivity upon indium enrichment, a key determinant of heat dissipation efficiency. Improved heat dissipation in copper based structures is also observed, underscoring the importance of microstructure control for enhancing thermal conductivity [28]. On the other hand, heat treatment processes such as homogenization and aging can significantly alter the microstructure of alloys which in turn improves their thermal properties. However, the addition of indium can complicate the alloy's fabrication and stability, which can hinder their deployment in real-world applications. Therefore, this study investigates the effect of indium addition (at 5 %, 10 %, and 15 % by weight) on the structural, thermal, and electrical properties of $Sn_{95}Al_5$ alloys. The primary objective is to identify the correlation between indium content, microstructure evolution, and the resulting macroscopic properties, thereby determining the optimal composition for enhanced performance as a lead-free solder material.

2. MATERIALS AND METHODS

Lead-free tin systems have demonstrated promising results in preliminary testing of new materials. Used alloys are made from metals that are 99.9 % pure or more. Tin, indium, and aluminum are some of these metals. In accordance with their weight percentages these metal mixtures are melted and cast onto substrates in air. Indium concentrations of 5, 10, and 15 wt.% were selected to systematically study the effect of a wide range of solute content on the microstructure and properties of the base $Sn_{95}Al_5$ alloy. The mixtures were melted in a furnace at 600 °C for 30 minutes under a nitrogen atmosphere to prevent oxidation, with constant stirring to ensure homogeneity. The molten alloy was then cast into a pre-heated (150 °C) steel mold. As demonstrated by Nawi et al. [29] in their analysis of aluminum alloy processing, controlled thermal conditions during casting are critical for achieving uniform microstructures, a principle applied here to ensure consistent Indium dispersion in Sn-Al alloys. Vickers hardness was measured using a 10-gram force applied for 5 seconds. The reported values are the average of 10 indentations taken on polished cross-sections of each alloy sample. The elastic modulus (E), shear modulus (μ), and bulk modulus (B) were determined from resonance frequency and damping analysis. A Shimadzu (Japan, Dx-30) X-ray diffractometer with 45 kV Cu-Ka radiation, 35 mA, nickel filters and an angular range of from 0 to 100° in continuous mode with a scan speed of 5 deg/min was used to analyze the samples. A Universal V4.5A TA instrument was used to create SC thermographs in the temperature range of 0 to 300 °C at a heating rate of 10 °C /min. A 20 kV, 10 mm SEM with a depth of field 300 times greater than optical microscopes was used for SEM analysis, and a JEOL JSM-6510 LV was used for microstructural characterization. To enable precise analysis of thermal properties like phase transition temperatures, enthalpy/entropy change values at phase transitions, etc., thermographs were created using differential scanning calorimetry (DSC) with a heating rate of 10 °C/min across a temperature range of 0 °C to 300 °C. Electrical resistivity was measured at room temperature (25 °C) using the four-point probe method to minimize contact resistance. Thermal conductivity (K) was calculated from the measured thermal diffusivity (D_{th}), specific heat capacity (C_p), and density (ρ) using the relationship $K = D_{th} * \rho * C_p$.

3. RESULTS AND DISCUSSION

3.1. X-ray diffraction

X-ray diffraction patterns of $Sn_{95-x}Al_5In_x$ (x = 5, 10, and 15 wt.%) alloys have lines corresponding to β- Sn and Al phases as shown in Fig. 1 – Fig. 4. These compounds help to alter the microstructure of the alloy, which, as supported by SEM images, leads to a refined grain structure and improves its mechanical properties. X-ray analysis shows that, adding In to $Sn_{95}Al_5$ alloy caused a change in the Sn matrix, such as lattice parameters and features of formed crystal structure (crystallinity, crystal size and orientation). That is because In dissolved in Sn matrix formed a solid solution, and other accumulated particles formed a trace of phases. Through the heterogeneous nucleation, indium addition leads to improved grain structure. The α-Al and β-Sn phases are formed by indium-rich clusters and primary interparticle, and this process simultaneously lowers the interfacial energy barrier required for nucleation, resulting in a finer

grain structure. It also improves the more homogeneous distribution of secondary phases enhance mechanical strength, and modifies thermal properties. The $Sn_{95}Al_5$ alloy exhibits a clear X-ray diffraction pattern with distinct peaks indicative of β-Sn phase, and the lattice parameters extracted from this pattern provide valuable information about the alloy's composition and structural integrity. Indium changes the lattice parameters of the β-Sn phase such that a solid solution within the tin matrix results. Furthermore, affecting the alloy's crystallinity is indium's presence.

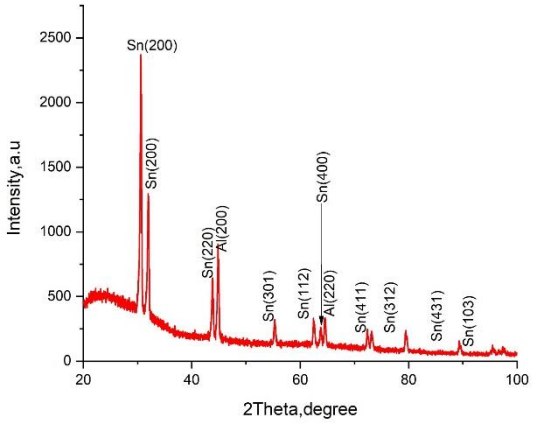


Fig. 1. X-ray diffraction pattern of $Sn_{95}Al_5$ alloy

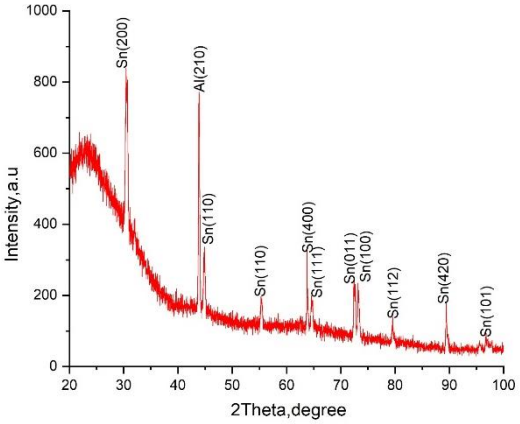


Fig. 2. X-ray diffraction pattern of $Sn_{90}Al_5In_5$ alloy

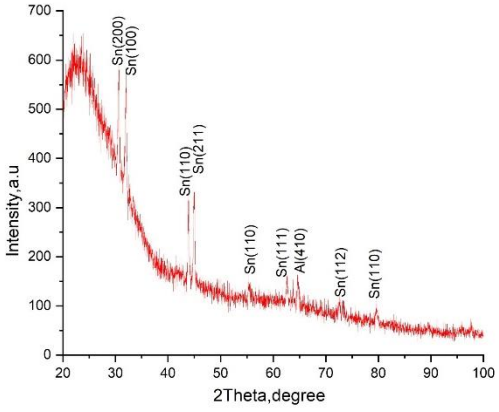


Fig. 3. X-ray diffraction pattern of $Sn_{85}Al_5In_{10}$ alloy

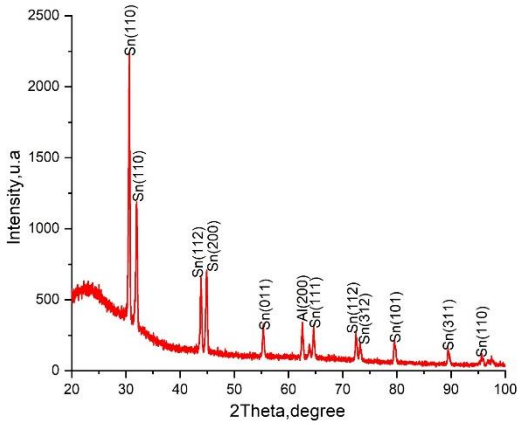


Fig. 4. X-ray diffraction pattern of $Sn_{80}Al_5In_{15}$ alloy

By higher indium content, extra peaks in the $Sn_{85}Al_5In_{10}$ alloy point to the creation of new phases brought on. The additional peaks at 2θ = 32.5°, 39.1° and 45.2° correspond to $InSn_4$ and AlIn inter-metallics. The $Sn_{80}Al_5In_{15}$ alloy exhibits a more noticeable change with several new peaks showing up. The microstructure of the alloy has changed, due to the rise in indium content to 15 wt.%, which generates extra intermetallic compounds. Intermetallic phases are formed when the solidification behavior of the $Sn_{80}A_{l5}In_{15}$ alloy is changed due to an increase in the indium content. These compounds help to alter the microstructure of the alloy, which in turn improves its mechanical properties and leads to a finer grain structure. These compounds improve the material's strength and hardness, but they make processing more difficult.

Table 1 shows the calculated lattice parameters, and the unit volume cell of the tetragonal tin phase in $Sn_{95}Al_5$ based alloy. From these results, lattice parameters and unit cell volume of the tetragonal tin phase changed related to alloys' structure, formed phases, after adding In element. The calculated crystal size (τ) shows some variation, which is attributed to differing levels of lattice strain and the influence of secondary phase formation on X-ray diffraction peak broadening, particularly in the $Sn_{85}Al_5In_{10}$ alloy.

Table 1. Lattice parameters, unit cell volume and crystal size of β-Sn in Sn95-xAl5Inx alloys

System, wt.%	*a*, Å	*c*, Å	*c*/*a*	*V*, Å^3	τ, Å
$Sn_{95}A_{l5}$	5.82	3.18	0.544	108.63	461.61
$Sn_{90}Al_5In_5$	5.87	3.11	0.526	106.41	390.43
$Sn_{85}Al_5In_{10}$	5.83	3.13	0.542	107.51	689.26
$Sn_{80}Al_5In_{15}$	5.81	3.15	0.542	108.09	432.52

Scanning electron micrographs, SEM, of $Sn_{95-x}Al_5In_x$ alloys show heterogeneity structure as shown in Fig. 5 – Fig. 7. SEM analysis of $Sn_{95-x}Al_5In_x$ alloys reveals properties consistent with previously obtained XRD findings. The heterogeneous grain structure observed in scanning electron microscopy images is consistent with the finding of Shahab et al. [30]. The effect of indium as an additive on the alloy morphology is very clear. The microstructure of Sn_{95}-x$A_{l5}In_x$ alloys also varies with the indium content. The initial effect of indium on the microstructure is clear in the heterogeneous structure of $Sn_{85}Al_5In_{10}$ alloy while $Sn_{85}Al_5In_{10}$ alloy exhibits a marked

change with a more homogeneous grain distribution, indicating improved crystallinity during solidification.

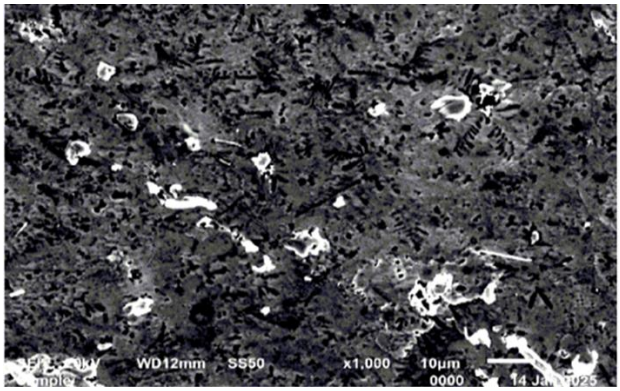


Fig. 5. Scanning electron micrograph of $Sn_{90}Al_5In_5$ alloy

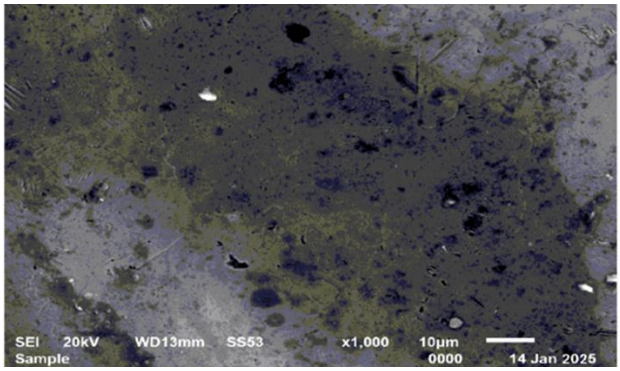


Fig. 6. Scanning electron micrograph of $Sn_{85}Al_5In_{10}$ alloy

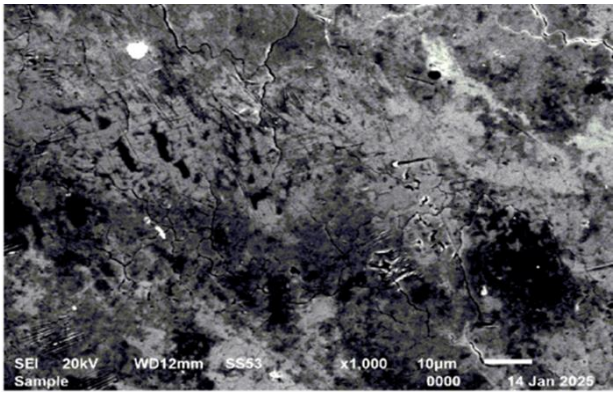


Fig. 7. Scanning electron micrograph of $Sn_{80}Al_5In_{15}$ alloy

This improved crystallinity leads to increased strength, and ductility, making the alloy's suitability for a wide range of applications. Moreover, clear evidence of the presence of intermetallic compounds resulting from indium addition indicates that the alloying process significantly modulates the phase composition. Rising indium content in the $Sn_{80}Al_5In_{15}$ alloy, most likely results in a finer grain structure and a change in intermetallic phases. These compounds might complicate processing but they can increase the hardness and strength of the material. However, the study was constrained by the relatively small range of indium concentrations tested, which may have prevented the detection of possible nonlinear effects at higher concentrations. To further optimize the properties of tin-aluminum-indium alloys future studies should investigate the effects of adding other alloying elements and expand the indium concentration range.

3.2. Mechanical properties

Elastic moduli of $Sn_{95-x}Al\ (In)_x$ alloys are listed in Table 2. Elastic modulus of $Sn_{95-x}Al_5\ (In)_x$ alloy varied after adding different ratios of Indium content. The $Sn_{80}Al_5In_{15}$ alloy has the highest elastic modulus.

Table 2. Elastic moduli, internal friction and thermal diffusivity of Sn95-xAl5Inx alloys

System, wt.%	E, GPa ±2%	μ, GPa ±2%	B, GPa ±2%	Q^{-1} ±10%	$D_{th}\times10^{-8}$ m^2/sec ±5%
$Sn_{95}Al_5$	31.71	11.71	37.38	0.012	11.81
$Sn_{90}Al_5In_5$	39.77	13.88	44	0.027	25.51
$Sn_{85}Al_5In_{10}$	38.81	14.29	45.4	0.024	6.196
$Sn_{80}Al_5In_{15}$	37.92	16	47.4	0.026	9.71

The DSC thermographs for $Sn_{95-x}Al_5In_x$ alloys are shown in Fig. 8 – Fig. 11. Internal friction of $Sn_{95}Al_5$ alloy increased after adding different ratio from Indium content. The $Sn_{90}Al_5In_5$ alloy has high internal friction value. This increase in hardness aligns with findings by Akopyan et al. [9], who reported significant hardening in Al-Si-Cu alloys with trace indium additions due to refined precipitation.

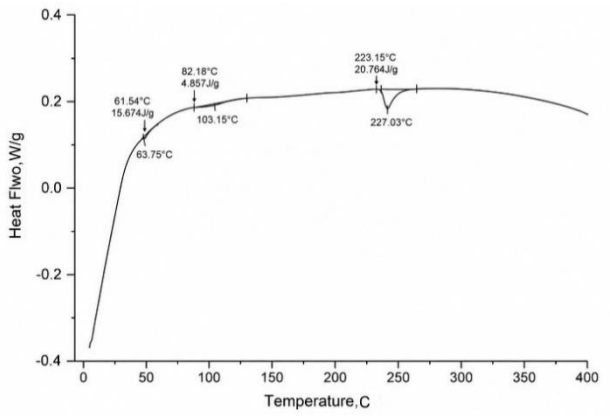


Fig. 8. DSC graph of $Sn_{95}Al_5$ alloy

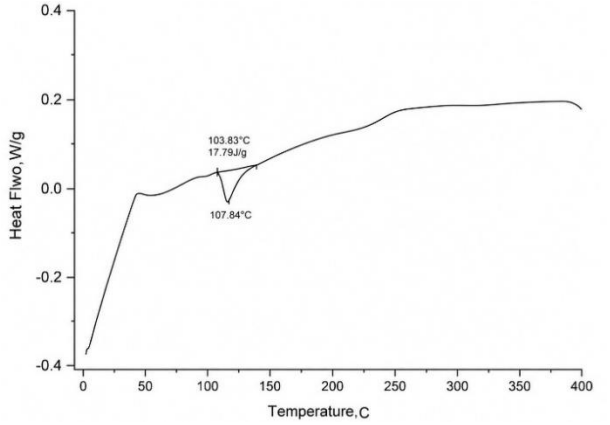


Fig. 9. DSC graph of $Sn_{90}Al_5In_5$ alloy

Vickers hardness of $Sn_{95-x}Al_5\ (In)_x$ alloys at 10-gram force and indentation time 5 sec are shown in Table 3. The slight decrease in Vickers hardness for the $Sn_{90}Al_5In_5$ alloy compared to the base $Sn_{95}Al_5$ alloy may be attributed to an initial solid solution softening effect, as indium atoms dissolve into the tin matrix [31].

Table 3. Vickers hardness and minimum shear stress of $Sn_{95-x}Al(In)_x$ alloys

System, wt.%	Hv, kg/mm^2	μ_n, kg/mm^2
$Sn_{95}Al_5$	36.43 ± 2.7	14.33
$Sn_{90}Al_5In_5$	35.77 ± 1.9	11.80
$Sn_{85}Al_5In_{10}$	37.88 ± 2.2	12.50
$Sn_{80}Al_5In_{15}$	38.92 ± 3.1	12.84
Trend with increasing In content (5 → 10 → 15 wt.%): Hv → (slight drop at 5 % then ↑); μn ↑ (overall).		

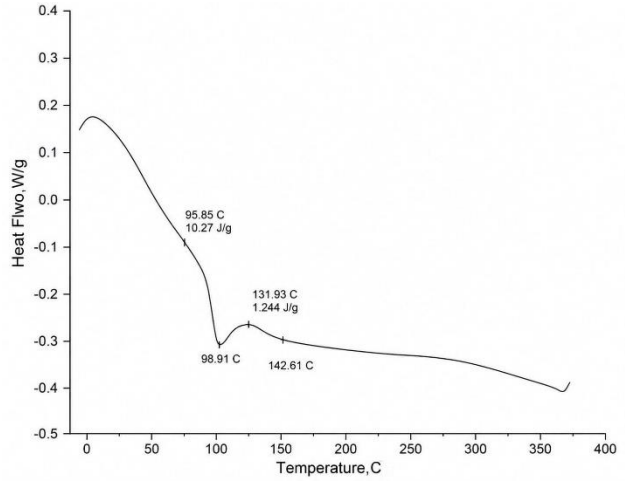


Fig. 10. DSC graph of $Sn_{85}Al_5In_{10}$ alloy

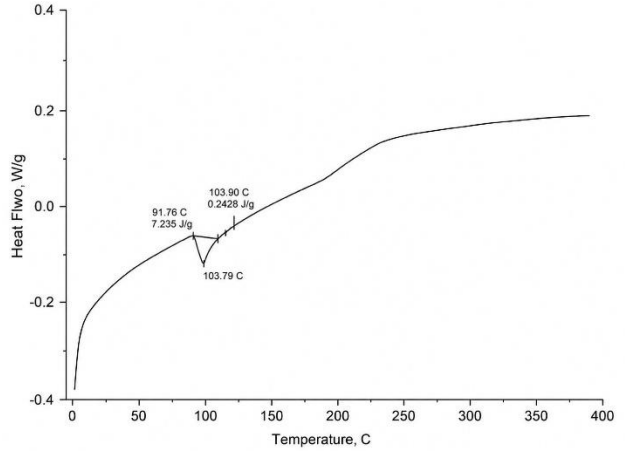


Fig. 11. DSC graph of $Sn_{80}Al_5In_{15}$ alloy

With higher indium content (10 and 15 wt.%), the increased formation of fine, hard intermetallic compounds overwhelms this effect, leading to a net increase in hardness. The minimum shear stress (τ_m) value of $Sn_{95-x}Al_5In_x$ alloys was calculated and then listed in Table 3.

Little variation occurred in the Vickers hardness of $Sn_{90}Al_5In_5$ alloy after Indium addition. Similar to the findings of Al Katawy et al. [2], where austempering techniques significantly enhanced hardness, the addition of Indium in Sn-Al alloys produced a comparable refinement in mechanical strength, as evidenced by increased Vickers hardness values.

3.3. Thermal and electrical properties

3.3.1. Thermal properties (DSC and thermal conductivity)

Fig. 8 – Fig. 11 show DSC thermographs for $Sn_{95-x}Al_5(In)_x$ alloys. A little variation occurred in the exothermal peak of $Sn_{95}Al_5$ alloy after Indium addition. The thermal behavior of the $Sn_{95}Al_5$ alloy is shown in the DSC graph, an exothermic peak denotes a phase transition. This graph provides a basis for comparison of the consequences of indium addition in later alloys. A small change in the exothermic peak of the $Sn_{90}Al_5In_5$ alloy indicates that indium addition has changed the alloy's thermal characteristics. This change is notable, since it influences the performance of the alloy in useful contexts. The more evident exothermic peak of the $Sn_{85}Al_5In_{10}$ alloy indicates additional changes in thermal behavior brought about by higher indium concentration. Higher than previous alloys this peak indicates a notable influence on melting temperature. The significant increase in the exothermic peak of the $Sn_{80}Al_5In_{15}$ alloy indicates significant changes in thermal properties with maximum indium concentration.
The advantages of $Sn_{95-x}Al_5Inx$ alloys mentioned above must be weighed against manufacturing challenges and stability considerations. Details of the melting point, and thermal behavior of these alloys are provided in Table 4, as well calculated internal friction and thermal diffusivity of $Sn_{99-x}Al_5In_x$ alloys are listed.

Research by Dawood et al. [7] indicates that adding 2 % by weight of indium to tin-bismuth alloys lowers the melting point from 139 °C to 114 °C, a significant difference of approximately 25 °C. As the indium content increases the melting point decreases further, requiring careful handling. This is a well-known thermodynamic phenomenon where increased indium leads to increased entropy and liquid-phase stability. This means the liquid phase becomes more stable than the solid phase at the same temperature as predicted by the tin-aluminum-indium three-phase diagram.

3.3.2. Electrical resistivity

As the indium content increases, the electrical resistivity increases due to electron scattering by indium atoms in the tin matrix. The $Sn_{95}Al_5$ alloy exhibits lower electrical resistivity compared to the $Sn_{90}Al_5In_5$ alloy. It is also observed that indium reduces thermal conductivity; the $Sn_{85}Al_5In_{10}$ alloy has a lower thermal conductivity than the $Sn_{95}Al_5$ alloy. Indium also enhances the electrical resistivity in Sn-Al-In alloys but improves the conductivity in $Sn_{43}Bi_{-2}In$ systems [7].

Table 4. Electric resistivity and other thermal properties of eutectic $Sn_{99-x}Al_5In_x$ alloys

System, wt.%	Melting point, ºC	Pasty range, °C	K, Wm^{-1}K^{-1} ±8%	C_p, J/g. ºC ±3%	ΔS, J/g. ºC ±4%	$\rho \times 10^{-6}$, Ω.cm ±2%
$Sn_{95}Al_5$	223.35	33.47	4.331	0.31	0.048	67.3
$Sn_{90}Al_5In_5$	107.94	19.07	4.504	0.92	0.157	137.30
$Sn_{85}Al_5In_{10}$	98.91	13.15	7.171	0.78	0.1	77.76
$Sn_{80}Al_5In_{15}$	94.08	11.24	3.552	0.64	0.074	68.40
- Trend with increasing In content: ρ ↑ at 5% then ↓; Tm ↓ progressively; K ↑ at 10% then ↓. - Measured by four-point probe, 1 mm spacing, 10 mA, 25 °C						

Furthermore, increasing the indium content lowers the melting points of these alloys, which can negatively impact heat management. Since the relationship between indium content, electrical resistivity, and thermal properties is complex, mechanical improvements may compensate for the negative effects of increased electrical resistivity and decreased thermal properties. Therefore, alloy design requires careful consideration to balance mechanical advantages with electrical and thermal performance. Thermal conductivity (K) and electrical conductivity (σ) in metals are often related by the Wiedemann-Franz law ($K/\sigma = LT$). However, in tin-aluminum-indium alloys, the marked increase in electrical resistivity at 5 % indium content is accompanied by only a slight change in thermal conductivity (from 4.33 to 4.50 W/m·K) because phonon scattering plays a dominant role. At higher indium content, the increased regularity of the microstructure leads to a decrease in both electrical resistivity and thermal conductivity due to the shift to a different scattering regime.

3.4. Microstructural-mechanical and thermal interrelation and its mechanical consequences

X-ray diffraction, SEM, differential thermal analysis (DSC), and mechanical testing combined demonstrate the effect of indium on the structure of the tin-aluminum alloy. DSC data show a gradual decrease in melting point with increasing indium content from 223.35 °C in pure $Sn_{95}Al_5$ to 94.08 °C in 15 wt.% indium, where it acts as an effective heat reducer, this suggests its potential use in heat sensitive applications like soldering on lithium batteries or electronic connectors. The lower melting point means faster cooling resulting in smaller and therefore denser crystals as confirmed by SEM images.

X-ray diffraction patterns indicate structural modification by indium addition. While the β-Sn phase remains dominant, changes in lattice parameters are observed. New diffraction characteristics appear at 10 – 15 wt.% indium indicating the formation of additional phases or changes in crystal arrangement [1, 3]. These structural changes are related to the microstructure enhancement previously observed in scanning electron microscopy (SEM) images. These changes explain the mechanical strengthening that was observed experimentally.

The mechanical results are consistent with the microstructure evolution. At 5 % indium, the indium acts as an alloy stabilizer interpenetrating the base metal atoms and causing a slight decrease in hardness, making the alloy more malleable and easier to work with. However, it also becomes weaker as some samples cracked. The transformation at 5 % occurs when the excess indium does not dissolve completely but forms secondary phases and new layers at the grain boundaries. These layers trap the grains, preventing them from growing into smaller grains and acquiring a stronger structure. The optimal point is at 15 %, where the best mechanical performance and fine microstructure are achieved, but there are some thermal stability issues, which limit its use in applications such as car engines.

Thermal diffusion data show a significant decrease in thermal conductivity when the indium content is increased by 10 wt.%. This decrease is attributed to the increased number of interfacial surfaces and phase boundaries, which act as thermal barriers. Conversely, increasing the indium content leads to a significant increase in the thermal diffusion of the alloy, which is directly related to grain smoothing and modified phase distribution, both of which significantly affect heat transfer efficiency, the results highlight the delicate balance in improving microstructure. It's not about blindly adding elements but about finding the optimal point where the benefits of particle smoothing outweigh the drawbacks of increasing particle boundaries. Electrical resistivity is a true reflection of changes occurring at the microstructure level. At 5 % indium resistivity increases significantly due to increased electron scattering from solute atoms and denser intermolecular boundaries, which act as additional barriers. However, as the indium content gradually increases, the situation reverses, and resistivity decreases because the structure becomes more ordered and the phases stabilize, allowing electrons to find smoother pathways compared to the disordered structure at lower indium concentrations.

To track the behavior of these alloys during heating, differential thermal scanning (DSC) provides comprehensive and detailed information. Lowering the melting point of indium not only facilitates the machining process but also improves grain fineness, which in turn enhances mechanical strength. X-ray diffraction (XRD) and scanning electron microscopy (SEM) confirmed the structural changes and provided evidence of these transformations. By combining the two analyses, the phases, morphology, and grain boundaries were identified, thus linking the thermal history to what is observed in the microstructure. Furthermore, the electrical and thermal conductivity properties indicate the effects of solid-solution formation, grain boundary density, and phase evolution. Therefore, based on the above, indium is not merely another alloying addition but a fundamental element for controlling the microstructure and improving the overall performance of lead-free tin-aluminum solder alloys.

4. CONCLUSIONS

The investigation into the impact of indium incorporation in tin-aluminum alloys has produced substantial revelations regarding the structural, thermal, and electrical characteristics of these materials, which are essential for their utilization in lead-free soldering. The experimental findings indicate that

1. The addition of indium (5 – 15 wt.%) to $Sn_{95}Al_5$ alloy induces microstructural refinement, as evidenced by SEM, and promotes the formation of intermetallic compounds, leading to an increase in Vickers hardness from 36.43 to 38.92 kg/mm² and a maximum elastic modulus of 37.92 GPa for the $Sn_{80}Al_5In_{15}$ alloy.
2. The thermal characteristics of the alloys with decreasing melting temperature by increasing indium content are much influenced by the indium content itself. A significant melting point depression from 223.35 °C to 94.08 °C was achieved, which is highly beneficial for low-temperature soldering applications.
3. Electrical resistivity showed a complex, non-monotonic relationship with indium content, initially increasing at 5 wt.% In and then decreasing, indicating a need for

careful compositional optimization to balance mechanical and electrical properties.

4. Indium promotes heterogeneous nucleation, resulting in finer, more uniformly sized grains, improving ductility and overall performance.
5. Future research should concentrate on optimizing indium content to maximize mechanical and thermal performance and investigating other alloying elements in concert with indium.

REFERENCES

1. **Shen, Y.A.** Effect of Indium Addition on Mechanical, Thermal, and Soldering Properties of Eutectic Sn–9Zn Alloy *Materials Chemistry and Physics* 315 2024: pp. 128992. https://doi.org/10.1016/j.matchemphys.2024.128992
2. **Al Katawy, A.A., Alrubaiy, A.A.A.G., Joma, A.J.S.** Enhancing Mechanical Properties of Low Alloy Steel through Novel Molten Bi-Ga Austempering. *Diyala Journal of Engineering Sciences.* 17 (2) 2024: pp. 173 – 181. https://doi.org/10.24237/djes.2024.17212
3. **Zhou, J., Shi, J., Yin, D., Xu, L., Zhang, F., Wang, Z., Hu, Q., Hu, H.** Investigation of the thermal properties, microstructure, and mechanical properties of Sn-3Ag-3Sb- *x* In lead-free solder alloys *Soldering & Surface Mount Technology* 37 (3) 2025: pp. 194 – 204. https://doi.org/10.1108/SSMT-11-2024-0068
4. **Sungkhaphaitoon, P., Chantaramanee, S.** Effects of Indium Content on Microstructural, Mechanical Properties and Melting Temperature of SAC305 Solder Alloys *Russian Journal of Non-Ferrous Metals* 59 (4) 2018: pp. 385 – 392. https://doi.org/10.3103/S1067821218040120
5. **Chantaramanee, S., Sungkhaphaitoon, P., Plookphol, T.** Influence of Indium and Antimony Additions on Mechanical Properties and Microstructure of Sn-3.0Ag-0.5Cu Lead Free Solder Alloys *Solid State Phenomena* 266 2017: pp. 196 – 200. https://doi.org/10.4028/www.scientific.net/SSP.266.196
6. **Chen, Z., Yan, K.** Grain Refinement of Commercially Pure Aluminum with Addition of Ti and Zr Elements Based on Crystallography Orientation *Scientific Reports* 10 (1) 2020: pp. 16591. https://doi.org/10.1038/s41598-020-73799-2
7. **Dawood, F., Al-Bawee, A.T., Alrubaiy, A.A.A.G.** Microstructural and Thermal Property Modifications of Sn-43Bi Solder Alloys via Selective Alloying with Se, In, Zn, and Al *Advances in Science and Technology Research Journal* 19 (8) 2025: pp. 273 – 284. https://doi.org/10.12913/22998624/205223
8. **Mostafa, A.O.** Mechanical Properties and Wear Behavior of Aluminum Grain Refined by Ti and Ti+B *International Journal of Surface Engineering and Interdisciplinary Materials Science* 7 (1) 2019: pp. 1 – 19. https://doi.org/10.4018/IJSEIMS.2019010101
9. **Akopyan, T.K., Belov, N.A., Letyagin, N.V., Milovich, F.O., Lukyanchuk, A.A., Fortuna, A.S.** Influence of Indium Trace Addition on the Microstructure and Precipitation Hardening Response in Al-Si-Cu Casting Aluminum Alloy *Materials Science and Engineering: A* 831 2022: pp. 142329. https://doi.org/10.1016/j.msea.2021.142329
10. **Mohammed, H.B., Naemah, I.M., Jomah, A.J.S., Alrubaiy, A.A.A.G.** Influence of Tool Pin Profile and Welding Parameters on Microstructure and Mechanical Properties of Dissimilar Friction Stir Welded AA2024 to AA7075 Alloys *Archives of Materials Science and Engineering* 124 (1) 2023: pp. 14 – 24. https://doi.org/10.5604/01.3001.0054.3228
11. **Wang, G., Sun, Q., Shan, L., Zhao, Z., Yan, L.** Influence of Indium Trace Addition on the Precipitation Behavior in a 357 Cast Aluminum Alloy *Journal of Materials Engineering and Performance* 16 (6) 2007: pp. 752 – 756. https://doi.org/10.1007/s11665-007-9086-3
12. **Shurkin, P.K., Akopyan, T.K., Letyagin, N.V.** Effect of Indium Microaddition on the Structure and Strengthening of Binary Al-Cu Alloy *Physics of Metals and Metallography* 122 (8) 2021: pp. 807 – 813. https://doi.org/10.1134/S0031918X21080159
13. **Yeh, C.H., Chang, L.S., Straumal, B.** Wetting Transition of Grain Boundaries in Tin–Rich Indium-Based Alloys and Its Influence on Electrical Properties *Materials Transactions* 51 (9) 2010: pp. 1677 – 1682. https://doi.org/10.2320/matertrans.M2010159
14. **Okle, P., Lin, J.D., Zhu, T., Dunand, D.C., Seidman, D.N.** Effect of Micro-Additions of Ge, In or Sn on Precipitation in Dilute Al-Sc-Zr Alloys *Materials Science and Engineering: A* 739 2019: pp. 427 – 436. https://doi.org/10.1016/j.msea.2018.10.058
15. **Kim, C.W., Cho, J.I., Choi, S.W., Kim, Y.C.** The Effect of Alloying Elements on Thermal Conductivity of Aluminum Alloys in High Pressure Die Casting *Advanced Materials Research* 813 2013: pp. 175 – 178. https://doi.org/10.4028/www.scientific.net/AMR.813.175
16. **Zhang, J., Gao, A.** Effect of Heat Treatment on Thermal Conductivity of 6063 Aluminum Alloy *In: 2011 Second International Conference on Mechanic Automation and Control Engineering IEEE* 2011: pp. 6449 – 6451. https://doi.org/10.1109/MACE.2011.5988519
17. **Lee, H.M., Bharathi, K., Kim, D.K.** Processing and Characterization of Aluminum Nitride Ceramics for High Thermal Conductivity *Advanced Engineering Materials* 16 (6) 2014: pp. 655 – 669. https://doi.org/10.1002/adem.201400078
18. **Ouyang, Y., Zhang, Z.** Advancing High Thermal Conductivity: Novel Theories, Innovative Materials, and Applications in Thermal Management Technologies *Journal of Physics: Condensed Matter* 36 (46) 2024: pp. 463002. https://doi.org/10.1088/1361-648X/ad7086
19. **Alhumairi, M.K.H.A., Yahya, S.G., Azzawi, I.D.J.** Experimental and Computational Investigation of Flame Holders in Combustion Chambers at Different Thermal Loads *Journal of Thermal Engineering* 6 (6) 2020: pp. 369 – 378.
20. **Stankus, S.V., Savchenko, I.V., Agazhanov, A.Sh.** Thermal Conductivity and Thermal Diffusivity of Liquid Indium-Tin Alloys *International Journal of Thermophysics* 33 (5) 2012: pp. 774 – 782. https://doi.org/10.1007/s10765-012-1192-2
21. **Peralta-Martinez, M.V., Wakeham, W.A.** Thermal Conductivity of Liquid Tin and Indium *International Journal of Thermophysics* 22 (2) 2001: pp. 395 – 403. https://doi.org/10.1023/A:1010714612865
22. **Shalaby, R.M., El-Sayed, M.** Effect of Heat Treatment on the Fracture and Structure of Tin-Indium Solder Alloy *Radiation Effects and Defects in Solids* 160 (1 – 2) 2005: pp. 23 – 31. https://doi.org/10.1080/10420150500032473
23. **Munther, M.** Effect of Adding Indium on Wetting Behavior, Microstructure and Physical Properties of Tin-Zinc Eutectic Alloy *International Journal of Science and Engineering Applications* 4 (4) 2015: pp. 186 – 191.

24. **Kim, S.K., Han, J.C., Seong, T.Y.** Thermally Stable Ti/Al-Based Ohmic Contacts to N-Polar n-GaN by Using an Indium Interlayer *Japanese Journal of Applied Physics* 55 (3) 2016: pp. 031001. https://doi.org/10.7567/JJAP.55.031001
25. **Mahlab, S.M., Kamal, M., Mansour, A.E.R.M.** Characterization of Indium Addition on Sn-Bi-Sb Lead-Free Solder Alloy *Journal of Advances in Physics* 12 (2) 2016: pp. 4231 – 4243. https://doi.org/10.24297/jap.v12i2.56
26. **Meydaneri Tezel, F., Saatçi, B., Arı, M., Durmuş Acer, S., Altuner, E.** Structural and Thermo-Electrical Properties of Sn-Al Alloys *Applied Physics A* 122 (10) 2016: pp. 906. https://doi.org/10.1007/s00339-016-0398-8
27. **Bakhtiyarov, S.I., Overfelt, R.A., Teodorescu, S.G.** Electrical Resistivity Measurements on Binary Al-15 wt-%In Alloy *Materials Science and Technology* 19 (3) 2003: pp. 322 – 326. https://doi.org/10.1179/026708303225010740
28. **Alrubaiy, A.A., Al-Bakri, B.A., Aljuhashy, R.M.** Thermal Performance of Double-Layer Porous Copper Strips Mounted as Hollow Cylinders *Periodicals of Engineering and Natural Sciences (PEN)* 9 (2) 2021: pp. 784 – 798. https://doi.org/10.21533/pen
29. **Nawi, S.A., Mohammed, H.B., Jasim, A.N., Sharaf, H.K., Muhammad, M.T.** Numerical Analysis of the Influence of the Rolling Speed on the Cold Rolling under Specific Thermal Condition of the AA 5052-O Aluminum Alloy *Journal of Advanced Research in Fluid Mechanics and Thermal Sciences* 122 (1) 2024: pp. 69 – 79. https://doi.org/10.37934/arfmts.122.1.6979
30. **Shehab, A.A., Nawi, S.A., Al-Rubaiy, A.A., Hammoudi, Z., Hafedh, S.A., Abass, M.H., Alali, M.S., Ali, S.D.** CO_2 Laser Spot Welding of Thin Sheets AISI 321 Austenitic Stainless Steel *Archives of Materials Science and Engineering* 2 (106) 2020: pp. 68 – 77. https://doi.org/10.5604/01.3001.0014.6974
31. **Zhou, S., Shen, Y.A., Uresti, T., Shunmugasamy, V.C., Mansoor, B., Nishikawa, H.** Improved Mechanical Properties Induced by In and In & Zn Double Additions to Eutectic Sn58Bi Alloy *Journal of Materials Science: Materials in Electronics* 30 (8) 2019: pp. 7423 – 7434. https://doi.org/10.1007/s10854-019-01056-y

© Dawood et al. *2026* Open Access This article is distributed under the terms of the Creative Commons Attribution 4.0 International License (http://creativecommons.org/licenses/by/4.0/), which permits unrestricted use, distribution, and reproduction in any medium, provided you give appropriate credit to the original author(s) and the source, provide a link to the Creative Commons license, and indicate if changes were made.